J Sol-Gel Sci Technol (2016) 80:411–416
DOI 10.1007/s10971-016-4110-4

ORIGINAL PAPER: SOL-GEL AND HYBRID MATERIALS FOR BIOLOGICAL AND HEALTH (MEDICAL) APPLICATIONS

Sol–gel synthesis and in vitro bioactivity of glass–ceramics in SiO_2–CaO–Na_2O–P_2O_5 system

Ashley Thomas[1] · **Japes Bera**[1]

Received: 12 March 2016 / Accepted: 6 June 2016 / Published online: 20 June 2016

Abstract Bioactive glass–ceramic powder in SiO_2–CaO–Na_2O–P_2O_5 system was successfully synthesised through a modified sol–gel route. The gel was prepared using tetraethyl orthosilicate, calcium nitrate, sodium nitrate and triethyl phosphate raw materials. The gel was calcined in the temperature range 700–1050 °C to get the glass–ceramic powder. Dissolution of the glass–ceramic powder was studied by in vitro immersion in Tris buffer solution for various period of time. The biodegraded powder was analyzed using XRD. The sintered glass–ceramic was characterized for in vitro bioactivity in simulated body fluid, and the incubated pellet was then analyzed for phase identification by XRD, surface morphology using SEM and elemental analysis using energy-dispersive X-ray analysis. The biocompatibility of the glass–ceramics was evaluated through MTT assay using MG-63 cells.

Graphical Abstract

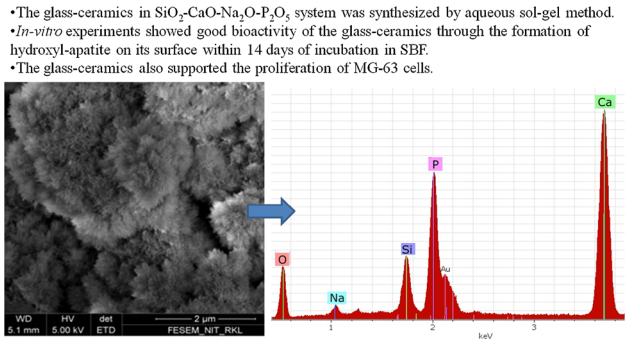

Keywords Biomaterials · Glass–ceramics · Sol–gel process · Bioactivity · Biocompatibility

1 Introduction

Bioactive glasses and glass–ceramics have found potential applications in tissue engineering where they are used as the template for the formation of a bioengineered tissue. They have been widely used in various medical fields like orthopedics, ENT, dentistry and maxillofacial applications [1–3]. The bioactive glass and glass–ceramics have the ability to interact with living tissue and to form bond with the bone, the behavior termed as bioactivity [3–5].

In spite of numerous advantages, bioactive glasses have low fracture toughness and are brittle [6–8]. One important approach to improve the mechanical properties of bioactive glass is its transformation into glass–ceramics, such as Cerabone®, A/W glass–ceramics [8–10]. Glass–ceramics materials which are formed by the partial crystallization of the base glass share many properties of both the glass and

✉ Japes Bera
jbera@nitrkl.ac.in

Ashley Thomas
ashleythomas88@yahoo.com

[1] Department of Ceramic Engineering, National Institute of Technology, Rourkela, Odisha 769008, India

the crystalline ceramics [11]. Glass–ceramics show similar bioactivity with that of the bioactive glass and have improved mechanical properties. Because of this, bioactive glass–ceramics are more suitable for different medical applications than the conventional bioactive glass implants.

The most commonly used method to produce glass–ceramics is the melt-quenching method. The method involves melting of the oxides at high temperatures, then quenching of the molten liquid to form the glass and subsequent annealing for partial crystallization of glass. But there are some problems associated with this method like; the processing temperature involved is higher than sol–gel processing route, and there are chances of contamination from the solid containers during high-temperature processing steps [12, 13]. The sol–gel method which was an alternative route proposed for bioactive glass synthesis by Li et al. [14] has several advantages and minimizes the limitations of the melt-quenching route. The method has better versatility compared to the melt-quenching technique and requires much lower processing temperatures [15–18]. The sol–gel bioactive glasses have nano-porosity which results in better cellular response and a better surface area hence better biodissolution. The major disadvantage of the sol–gel process is the requirement of high-purity raw materials which are expensive in general. Conventional sol–gel processing is acidic hydrolysis and then leaving the sol to gel.

Glass–ceramics in SiO_2–CaO–Na_2O–P_2O_5 system have been reported by many authors [10, 12, 19–31]. Among them, majority are by melt-quenching method [10, 19–24]. There are some reports in sol–gel synthesis [12, 25–31]. Although there is no requirement of Na_2O in sol–gel glass as its role in traditional glass synthesis is to lower the melting point, it is employed in various sol–gel-based bioactive glasses because it improves the solubility of glass in aqueous media and it offers advantages during crystallization of the glass through heat treatment [13, 30]. Crystallization treatment is applied to improve the mechanical strength of glass and to get glass–ceramics. Recently, a partially crystallized glass–ceramics (GC) composition in SiO_2–CaO–Na_2O–P_2O_5 system has been synthesized which shows a significantly greater flexural strength than cortical bone, at the same time showing a very high bioactivity and much lower elastic modulus compared to Cerabone® [10]. This GC also shows a similar level of bioactivity to the golden standard 45S5 bioglass®, and all these can be attributed to the formation of $Na_2Ca_2Si_3O_9$ crystalline phase in the glass–ceramics. The crystallization and sintering behavior of the same GC has recently been reported by the present authors [32].

Similar GC composition has been synthesized through sol–gel method using two different raw materials for phosphate: triethyl phosphate and phosphoric acid [12]. However, the authors concluded that the GC containing only $Na_2Ca_2Si_3O_9$ crystalline phase could not be obtained in case of triethyl phosphate raw material. Hence, a modification of the sol–gel method is required to obtain $Na_2Ca_2Si_3O_9$ phase when the triethyl phosphate raw material is used for the synthesis. In the present investigation, a modified sol–gel route similar to that proposed by Chen et al. [30] is used to synthesize the GC with the same composition reported by Peitl et al. [10] using triethyl phosphate raw material. A highly bioactive GC containing only $Na_2Ca_2Si_3O_9$ crystalline phase has been achieved. The bioactivity, biocompatibility and the dissolution behavior of the GC have been investigated.

2 Materials and methods

The GC with the composition (in mol%) SiO_2—49.2, Na_2O—23.4, CaO—25.5 and P_2O_5—1.7 was prepared by sol–gel process. High-purity regent grade tetraethyl orthosilicate (TEOS, Alfa Aesar), triethyl phosphate (TEP, Alfa Aesar), sodium nitrate (MERCK) and calcium nitrate tetrahydrate (NICE Chemical) were used for the synthesis. The sol–gel synthesis was carried out using a procedure described elsewhere [30]. Briefly, the precursors TEOS, TEP, $NaNO_3$ and $Ca(NO_3)_2$ were taken according to the required molar ratio of SiO_2, P_2O_5, Na_2O and CaO stated above for the GC composition. The molar ratio of water/precursor chemical was taken 10 to achieve a clear sol. The precursors were added slowly into the HNO_3 aqueous solution in the sequence: TEOS, TEP, Ca $(NO_3)_2$ and $NaNO_3$ with constant stirring condition; each was added only after the sol became clear. The final sol was kept at ambient condition for gelling. The resulting gel was dried at 60 °C for 3 days and calcined at 700 °C for 2 h.

GC powders were characterized for crystalline phase identification using X-ray diffraction (XRD) analysis. Microstructure of specimen was characterized using thermal field emission gun scanning electron microscope (FESEM, FEI). Elemental analysis of specimen was carried out using energy-dispersive X-ray (EDX) spectra equipped with the FESEM.

2.1 In vitro biodegradation studies

In vitro biodegradation behavior of GC was evaluated by soaking the GC powder in Tris buffer solution (TRIS-BS) and measuring the change in pH of the BS with time [33]. In short, 0.3 g of GC powder was dispersed in 200 ml of TRIS-BS. The initial pH was kept to 7.78 to 8 as the maximum buffer capacity for TRIS-BS is 8.0. The change in pH was studied as a function of material incubation time at 37 °C for 5 days. After this incubation period, the suspension was filtered through Millipore filters. The solid component was dried in air and analyzed by XRD.

2.2 In vitro bioactivity studies

Bioactivity or the bone bonding ability of a material to host bone is associated with the formation of a carbonated hydroxyapatite layer on the surface of the material when in contact with biological fluids. The ability of GC to bond with bone can be assessed in vitro in simulated body fluid (SBF) by monitoring the formation of hydroxyapatite on its surface. SBF was prepared as per the ISO standard reference no ISO/FDIS 23317:2007(E). The sintered GC pellets were immersed in SBF in flasks. The flasks were kept inside an incubator at 37 °C. The pellets were removed from the SBF solution after given times of 14 and 28 days. The SBF was replaced every week because the cation concentration of SBF solution changes during the course of experiments as a result of changes in chemical compositions of the samples. Once removed, the samples were rinsed in deionized water and left to dry at ambient temperature in desiccators. The samples were characterized using X-ray diffraction analysis (XRD), FESEM and EDX to assess the possible formation of hydroxyapatite upon the surface of GC.

2.3 Cell viability assay

The biocompatibility studies were performed using MG-63 cell line, procured from NCCS, Pune. The cells were maintained in Dulbecco's modified Eagle's medium (DMEM) with 10 % fetal bovine serum (FBS) at 37 °C, with 5 % CO_2 and 95 % humidity environment. The GC samples were normalized by incubating in cell culture medium for 48 h. After the incubation, centrifugation was carried out, the media was decanted, and fresh 1 ml DMEM was added for leaching. While passaging, the cells were washed and harvested using 1× Dulbecco's phosphate buffer saline and trypsin–EDTA solution, respectively. The viable cell density in the harvested culture was accessed using trypan blue dye exclusion test, and the cells were then seeded onto a 96-well plate at a cell concentration of 5×10^4 cells/ml. The seeded plate was kept in incubator for next 12 h for adherence. After that, cells were incubated with the samples at a concentration of 10 µg/ml for period of 24 h. After incubation period, the cell viability index was accessed using MTT assay. Statistical significance was assessed by single-way ANOVA, and '*p*' value <0.05 was considered significant.

3 Results and discussion

Figure 1 shows the XRD patterns of the gel and calcined GC powder. The crystalline phase in dry gel was identified to be sodium nitrate (PDF #79-2056). There was an amorphous phase also in the gel. The presence of sodium nitrate phase in the gel has been reported earlier and explained that the gel should be stabilized at a temperature higher than 600 °C for the complete removal of nitrogen containing compounds [31, 32]. The phases in 700 °C calcined powder were identified to be $Na_2Ca_2Si_3O_9$ (combeite) (PDF #77-2189) and $Na_8Ca_3Si_5O_{17}$ (PDF #10-0053). However, the crystalline phase in 1000 °C calcined GC was identified to be solely combeite (Fig. 1c). No phosphate-based ceramics phase was identified. Phosphorus ions might be present as solid solution in combeite phase or in residual glass phase as minor fraction.

The dissolution behavior of GC powders is evaluated by soaking in different aqueous media like deionized water, phosphate-buffered saline (PBS), SBF or TRIS-BS. In this investigation, TRIS-BS was used as soaking medium. Figure 2 shows the change in pH of the TRIS-BS during dissolution of GC powder. The figure shows that the pH of the solution increases with soaking time and a saturate state pH was obtained after 3-day soaking. The largest increase in pH was observed during first 8 h. The increase in pH is due to the leaching out of Na^+ and Ca^{2+} ions from the GC. These cations are exchanged with H^+ ions from the solution. Initial quick increment in pH value was due to the fast release of mainly Na^+ ions [29]. The ion release (pH increment) was slower in 1050 °C calcined specimen compared to 1000 °C calcined product. The slower ion release may be due to the bigger grain size and lower grain boundary area in 1050 °C calcined GC as shown in the inset of Fig. 2.

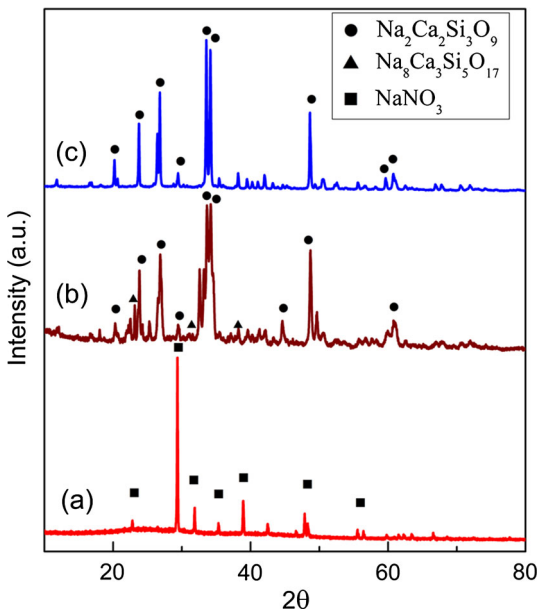

Fig. 1 XRD patterns of (*a*) gel powder dried at 60 °C, glass ceramics powder obtained by calcinations of gel at (*b*) 700 °C and (*c*) 1000 °C for 2 h

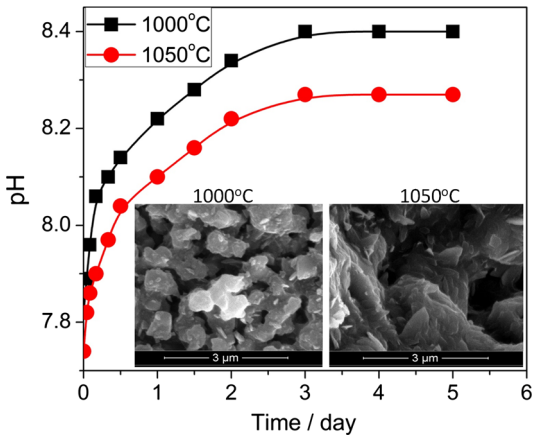

Fig. 2 pH as a function of incubation time in Tris-buffered solution for glass–ceramics powders fired at 1000 and 1050 °C, respectively

Figure 3 shows the XRD patterns of GC powders after 3 days of degradation test. The figure shows that the combeite phase peaks height decreases after incubation due to the dissolution of the phase. The combeite phase was relatively more in 1050 °C calcined sample due to the slower degradation rate of the specimen. Amorphous patterns were observed in both cases due to the depletion of crystalline phase combeite from the surface of the GC. The major phase deposited during the process was calcium carbonate. The formations of amorphous pattern along with the increase in pH of the TRIS-BS are the strong evidence of the high biodegradability of the GC. The sol–gel method of GC preparation could be the reason for high biodegradability of it.

Figure 4 shows the XRD pattern of GC pellet after soaking in SBF solution for different days. XRD pattern shows an amorphous phase along with combeite and $CaCO_3$ phases. The amorphous phase becomes prominent due to the depletion of crystalline combeite phase from the surface through dissolution. $CaCO_3$ deposition on the surface was due to the absorption of CO_2 from atmosphere. The amount of combeite phase decreased with increasing incubation time, and it disappeared after 28 days. The apatite phases along with calcium carbonate were observed after 14 days. The apatite phase precipitation phenomenon confirms the high solubility and ion exchange capability behavior of the GC. The formation of apatite indicates that the material has good bonding ability.

FESEM-EDX analysis was carried out to evaluate the morphology and composition of apatite formed. Figure 5 shows morphology and elemental mapping of pure GC and after soaking in SBF solution. Un-treated GC micrograph shows grains in the size range 1–2 micron, and EDX shows mainly Na–Ca-silicate phase with minor P element in solid solution. Fourteen-day incubated specimen microstructure shows the formation of flowery like apatite on the surface of GC. The size of apatite crystals and their concentration increased with incubation time in SBF. Compared to the untreated pellets which showed a higher concentration of Si and a very low concentration of P, the SBF soaked pellets showed high concentrations of Ca and P, confirming the formation of apatite on the surface of the GC.

The cyto-compatibility of the GC material was investigated using MG-63 cells in the standard culture medium

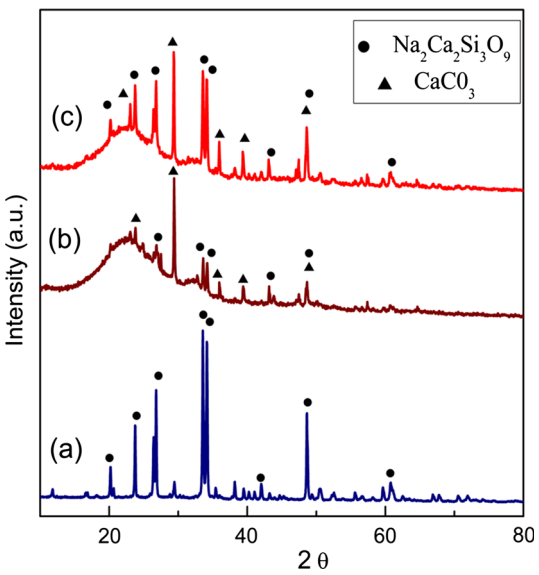

Fig. 3 X-Ray diffraction patterns of GC powders (*a*) after calcinations at 1000 °C, and after 3-day soaking in Tris-buffered solution for (*b*) 1000 °C and (*c*) 1050 °C calcined powders

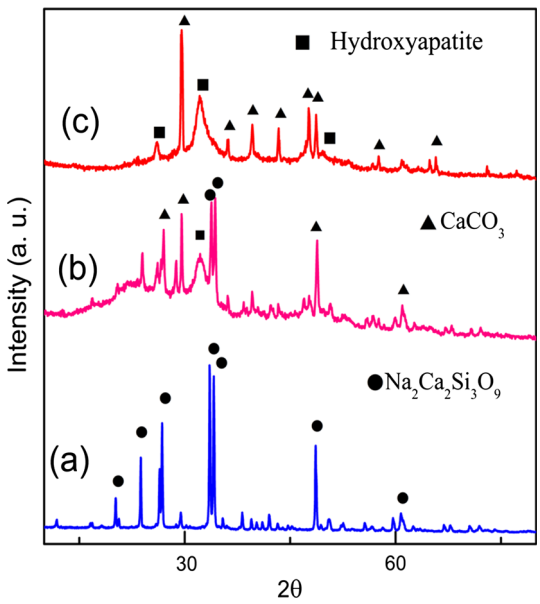

Fig. 4 X-Ray diffraction patterns of sol–gel-derived glass–ceramics pellets (*a*) sintered at 1000 °C, after immersion in SBF solution (*b*) for 14 days and (*c*) for 28 days

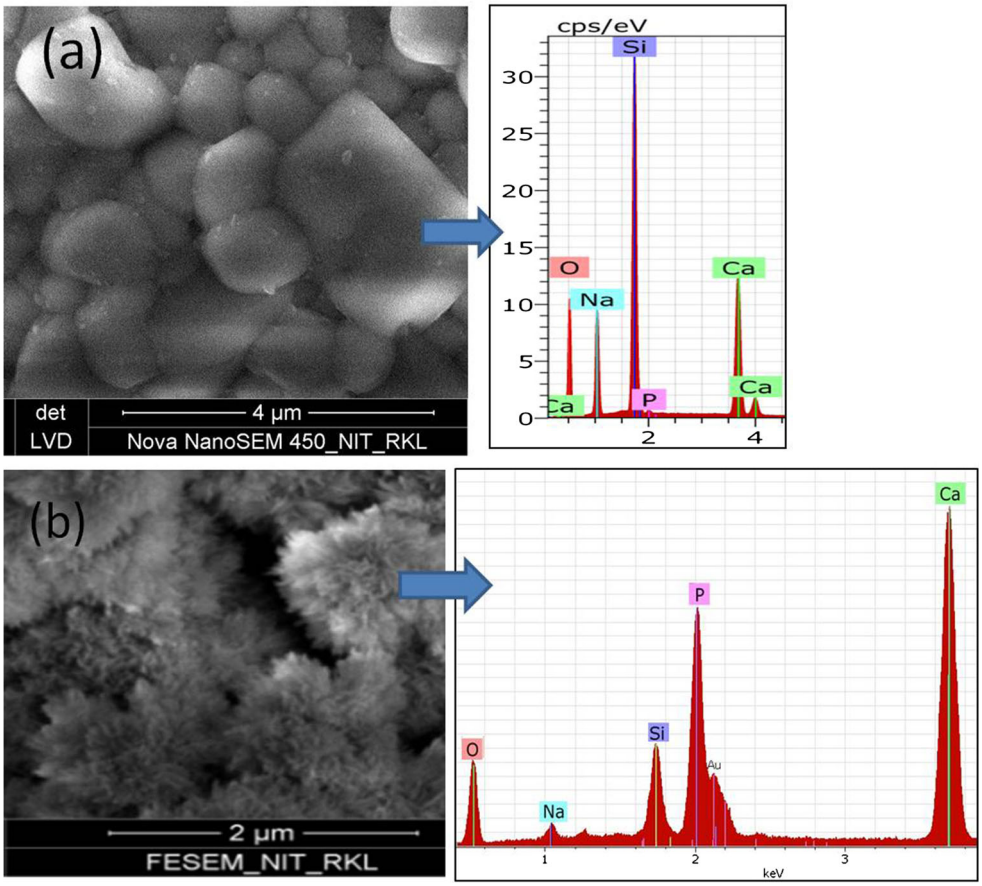

Fig. 5 FESEM image and EDX spectra of **a** untreated GC pellet and **b** GC after soaking in SBF solution for 14 days

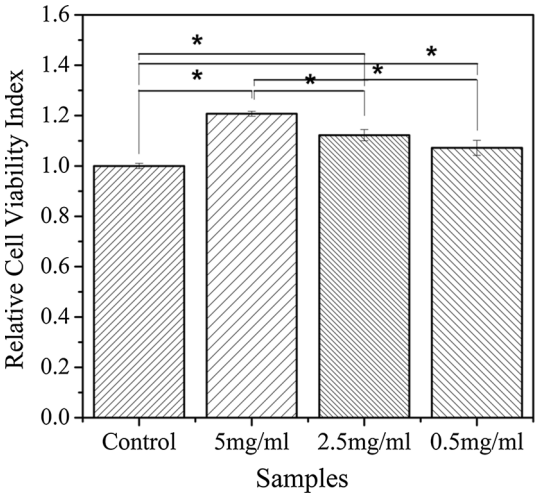

Fig. 6 Cell viability index of different concentrations of GC samples (0.5, 2.5 and 5 mg/ml) and the negative control. The data are expressed as mean ± SD ($n = 3$), and the statistical significance is assessed (*$p < 0.05$)

using the MTT assay. Figure 6 shows the cell viability index of different concentrations of GC powder samples (0.5, 2.5 and 5 mg/ml) and the negative control. The culture medium containing the extracts of GC powders was found to support proliferation of MG-63 cells, and microscopic observation showed no significant morphological differences between the negative control and the samples of different concentrations. The MTT assay of the samples showed that all GC samples enhance the proliferation of MG-63 cells compared with control as evident from the cell viability index graph (Fig. 6) and variation was found to be statistically significant in all the GC samples ($p < 0.05$) compared to the control. The cell proliferation was found to increase with concentration of GC sample, and the sample with concentration of 5 mg/ml GC showed highest proliferation (that is a higher cell viability index). Hence, these data are a quantitative confirmation of the excellent biocompatibility of the material.

4 Conclusions

Bioactive glass–ceramic powder in SiO_2–CaO–Na_2O–P_2O_5 system was synthesized by an aqueous sol–gel method. The gel stabilization temperature was 700 °C. Firing of gel leads to the formation of combeite as the main crystalline phase in the GC. The GC containing only combeite phase ($Na_2Ca_2Si_3O_9$) was achieved by heat treatment at 1000 °C

for 2 h. The dissolution behavior of the GC was found to depend on their heat treatment temperature, and dissolution rate of GC decreased with increase in heat treatment temperature. The GC showed good bioactivity by forming hydroxyapatite on the surface within 14 days of incubation in SBF through quick release of alkaline ions. Good bioactivity of the GC was owing to the high surface area and porous structure of GC produced by the sol–gel method. The sol–gel-derived GC also supported the proliferation of MG-63 cells.

Acknowledgments This research was financially supported by National Institute of Technology, Rourkela, India.

References

1. Hench LL (2006) The story of bioglass. J Mater Sci Mater Med 17:967–978
2. Gerhardt LC, Boccaccini AR (2010) Bioactive glass and glass–ceramic scaffolds for bone tissue engineering. Materials (Basel) 3:3867–3910
3. Hench LL, Wheeler DL, Greenspan DC (1998) Molecular control of bioactivity in sol–gel glasses. J Sol-Gel Sci Technol 13:245–250
4. Hench LL, Wilson J (1993) An introduction to bioceramics. World Scientific, Singapore
5. Hench LL, Splinter RJ, Allen WC, Greenlee TK (1971) Bonding mechanisms at the interface of ceramic prosthetic materials. J Biomed Mater Res 5:117–141
6. Rezwan K, Chen QZ, Blaker JJ, Boccaccini AR (2006) Biodegradable and bioactive porous polymer/inorganic composite scaffolds for bone tissue engineering. Biomaterials 27:3413–3431
7. Jones JR, Clare AG (2012) Bio-glasses: an introduction. Wiley-Blackwell, New York
8. Fu Q, Saiz E, Rahaman MN, Tomsia AP (2013) Toward strong and tough glass and ceramic scaffolds for bone repair. Adv Funct Mater 23:5461–5476
9. Kokubu T (1991) Bioactive glass ceramic: properties and application. Biomaterials 12:155–163
10. Peitl O, Zanotto ED, Serbena FC, Hench LL (2012) Compositional and microstructural design of highly bioactive P_2O_5–Na_2O–CaO–SiO_2 glass–ceramics. Acta Biomater 8:321–332
11. Höland W, Beall GH (2012) Glass–ceramic technology, 2nd edn. Wiley, New York
12. Siqueira RL, Peitl O, Zanotto ED (2011) Gel-derived SiO_2–CaO–Na_2O–P_2O_5 bioactive powders: synthesis and in vitro bioactivity. Mater Sci Eng C 31:983–991
13. Jones JR (2013) Review of bioactive glass: from Hench to hybrids. Acta Biomater 9:4457–4486
14. Li R, Clark AE, Hench LL (1991) An investigation of bioactive glass powders by sol–gel processing. J Appl Biomater 2:231–239
15. Sepulveda P, Jones JR, Hench LL (2001) Characterization of melt-derived 45S5 and sol–gel derived 58S bioactive glasses. J Biomed Mater Res 58:734–740
16. Li R, Clark AE, Hench LL (1991) Alkali-free bioactive sol–gel compositions. Patent International WO1991/017965
17. Sakka S (2005) Handbook of sol–gel science and technology: processing, characterization and applications, vol 1. Kluwer, Dordrecht
18. Hong Z, Liu A, Chen L, Chen X, Jing X (2009) Preparation of bioactive glass–ceramics nanoparticles by combination of sol–gel and coprecipitation method. J Non-Cryst Solids 355:368–372
19. Plewinski M, Schickle K, Lindner M, Kirsten A, Weber M, Fischer H (2013) The effect of crystallization of bioactive bioglass 45S5 on apatite formation and degradation. Dent Mater 29:1256–1264
20. Kashyap S, Griep K, Nychka JA (2011) Crystallization kinetics, mineralization and crack propagation in partially crystallized bioactive glass 45S5. Mater Sci Eng C 31:762–769
21. Guillon O, Cao S, Chang J, Wondraczek L, Boccaccini AR (2011) Effect of uniaxial load on the sintering behaviour of 45S5 Bioglass® powder compacts. J Eur Ceram Soc 31:999–1007
22. Chen QZ, Efthymiou A, Salih V, Boccaccini AR (2008) Bioglass-derived glass–ceramic scaffolds: study of cell proliferation and scaffold degradation in-vitro. J Biomed Mater Res A 84:1049–1060
23. Teixeira LN, Ravagnani C, Peitl O, Zanotto ED (2007) In-vitro osteogenesis on a highly bioactive glass–ceramic. J Biomed Mater Res Part A 82:545–557
24. Li HC, Wang DG, Hu JH, Chen CZ (2013) Crystallization, mechanical properties and in vitro bioactivity of sol–gel derived Na_2O–CaO–SiO_2–P_2O_5 glass–ceramics by partial substitution of CaF_2 for CaO. J Sol-Gel Sci Technol 67:56–65
25. Rezabeigi E, Wood-Adams PM, Drew RAL (2014) Synthesis of 45S5 Bioglass® via a straightforward organic, nitrate-free sol–gel process. Mater Sci Eng C Mater Biol Appl 40:248–252
26. Catteaux R, Grattepanche-Lebecq I, Désanglois F, Chai F, Hornez JC, Hampshire S et al (2013) Synthesis, characterization and bioactivity of bioglasses in the Na_2O–CaO–P_2O_5–SiO_2 system prepared via sol gel processing. Chem Eng Res Des 91:2420–2426
27. Lucas-Girot A, Mezahi FZ, Mami M, Oudadesse H, Harabi A, Le Floch M (2011) Sol–gel synthesis of a new composition of bioactive glass in the quaternary system SiO_2–CaO–Na_2O–P_2O_5. J NonCryst. Solids 357:3322–3327
28. Han X, Li X, Lin H, Ma J, Chen X, Bian C, Wu X, Qu F (2014) Hierarchical meso–macroporous bioglass for bone tissue engineering. J Sol-Gel Sci Technol 70:33–39
29. Chen QZ, Thompson ID, Boccaccini AR (2006) 45S5 Bioglass-derived glass–ceramic scaffolds for bone tissue engineering. Biomaterials 27:2414–2425
30. Chen QZ, Li Y, Jin LY, Quinn JMW, Komesaroff PA (2010) A new sol–gel process for producing Na_2O-containing bioactive glass–ceramics. Acta Biomater 6:4143–4153
31. Pirayesh H, Nychka J (2013) Sol–gel synthesis of bioactive glass–ceramic 45S5 and its in vitro dissolution and mineralization behavior. J Am Ceram Soc 96:1643–1650
32. Thomas A, Bera J (2016) Crystallization and sintering behavior of glass–ceramic powder synthesized by sol–gel process. J Austr Ceram Soc 52(2):1–5
33. Cerruti MG, Greenspan D, Powers K (2005) An analytical model for the dissolution of different particle size samples of Bioglass in TRIS-buffered solution. Biomaterials 26:4903–4911